Design of a Movable Palm Fruit Bunch Stripper for Oil Extraction

Undiandeye, Sylvester Akwagiobe[1], Markson, I. E.[2], Offiong, Alexander Aniekan[3], Offiong Aniekan[4], and A.P. Ihom[5]
Department of Mechanical Engineering
University of Uyo, Uyo Akwa Ibom State, Nigeria
Corresponding Author: draondonaphilip@gmail.com
DOI: 10.56201/ijcsmt.v10.no4.2024.pg175.193

Abstract
In this paper, the design of a movable palm fruit bunch stripper (MPFBS) plant for oil extraction is presented. The palm fruit bunch stripper designed in this work has the following components: the main frame and metal base, the beaters, the shaft, the bearings, the belt, the pulleys, the electric motor, the generator, the stripping chamber, the fruitlet screen, the bolt and nut and the gear reduction box. Specifically, the design details are broken down into the following subsections, the power requirement for stripping process, selection of electric motor/generator and torque, transmission drive design, design of stripping chamber shaft, key and keyway design, design of bolts and nuts, fruitlet screen design, stripping chamber design and frame design. Detailed analytical expressions for the computation of the design parameters in each of the subsections are presented and then sample design calculations were conducted using Customized M236 Machine Design Spreadsheet, powered by Microsoft Excel®. According to the sample simulation results, two bunches of palm fruits each weighing 40 kg were considered and the power expected for the stripping process was 2.218 kW or 2.98 hp. Furthermore, the electric motor power supply (to be chosen) is 5.33 hp, the speed from gear box is 100 rpm and the torque on shaft or the machine pulley required is 284.53 N-m.

Keywords: *Palm Fruit Bunch Stripper, Customized M236 Machine Design Spreadsheet, Oil Extraction, Stripping Chamber Shaft, Palm Fruit*

1.0 Introduction

The oil palm tree (Elaeis guineensis) is a superb economic and perennial plant (Babu, Mathur, Anitha, Ravichandran and Bhagya, 2021; Mayes, 2020; Pinnamaneni and Potineni, 2022). Tropical regions are its natural habitat (Asbur, Purwaningrum and Ariyanti, 2020; Adade, 2022; Gan, Teo, Manirasa, Wong and Wong, 2021). Although produced commercially throughout Southeast Asia and Southern America, its origins may be traced back to Africa, primarily the southern regions of Ghana and Nigeria. It grows in warm climate zones at elevations of 500 m above sea level and bears fruits in bunches that weigh 10 to 40 kg (Nair and Nair, 2021; Oteng, 2020; Oshiobugie *et al.*, 2017; Assian *et al.*, 2022).

The ideal oil palm bunch, consists of 60.0–65.0% fruits, 21.0–23.0% palm oil, 5.0–7.0% kernel, and 44.0–46.0% mesocarp (Assian *et al.*, 2022). After being picked, the palm fruits go

through a number of processing steps, including bunch reception, threshing (stripping or detaching), sterilisation (heating the fruits), digestion (pounding), palm oil extraction/clarification, nut-fibre separation, nut drying and cracking, kernel separation, and crushing and pressing of the kernels. However, there are two approaches. The traditional process of stripping the fruit bunch (FB) takes a long time and produces little palm oil, according to Oshiobugie *et al.* (2017). On the other hand, mechanized palm fruit bunch strippers have been developed. However, there are some limitations such low cleaning, stripping efficiencies, among others. Accordingly, careful selection of design parameters and use of appropriate analytical model and machine design principles can be used to address some of the issues associated with the mechanized palm fruit bunch strippers. Accordingly, in this work, the design of a movable palm fruit bunch stripper for efficient oil extraction is presented. The major machine components were identified and several mathematical models and standard engineering principles were employed in the analytical design of the machine parts using Customized M236 Machine Design Spreadsheet (Olosunde, Assian and Antia, 2023; Antia, Assian and Ukaru, 2021).
The objective of this work is to design a movable palm fruit bunch stripper for oil extraction; this will reduce the processing time for oil extraction and labour expended in extracting palm oil.

2.0 Materials and Method

2.1 Design Analysis and Calculations for palm fruit bunch stripper

The palm fruit bunch stripper designed in this work has the following components: the main frame and metal base, the beaters, the shaft, the bearings, the belt, the pulleys, the electric motor, the generator, the stripping chamber, the fruitlet screen, the bolt and nut and the gear reduction box. Specifically, the design details are broken down into the following subsections, the power requirement for stripping process, selection of electric motor/generator and torque, transmission drive design, design of stripping chamber shaft, key and keyway design, design of bolts and nuts, fruitlet screen design, stripping chamber design and frame design.

2.1.1 Power Requirement for Stripping Process (P_{sp})

(a) Weight of n-Number of Oil Palm Fruit Bunch

Weight of n-number of oil palm fruit bunch in the hopper (W_{nf}) is computed as:

$$W_{nf} = n_f \,.\, m_{fb} \,.\, g \qquad (1)$$

Where, n_f = number of oil palm fruits bunches, m_{fb} is the mass of oil palm fruit bunch in the hopper and g = acceleration due to gravity (9.81 m.s^{-2}).

(b) Volume of a Beater Blade (V_{bb})

The **volume of a beater blade** is computed as:

$$V_{bb} = h.\, b.\, l \qquad (2)$$

Where, h = height of beater blade (m), b = base of beater blade (m) and *l* = length of beater blade (m).

(c) Total Number of Beater blades on the Shaft ($t_{-blades}$)

Total number of beater blades on the shaft ($t_{-blades}$) is derived from:

$$t_{-blades} = n_{-spot} \,.q \qquad (3)$$

Where, n_{-spot}= number of spot where beaters are located and q = number of beater blades per spot.

(d) Weight of Total Number of Beater Blades ($W_{t-blades}$)

Weight of total number of beater blades ($W_{t-blades}$) is computed as :

$$W_{t-blades} = V_{bb} \times \rho \times g \times t_{-blades} \quad (4)$$

Where, ρ = density of beater blade (mild steel) and g = 9.81 $m.s^{-2}$

(a) Max Load Key on the Shaft ($W_{max.s}$)

If the stripping force of palm fruit after 24 hours of storage (F_{sp}) was reported as 300 N by (Olotu *et al.* 2020), then, the maximum load key is computed as :

$$W_{max.s} = W_{nf} + W_{t-blades} + F_{sp} \quad (5)$$

The power requires for stripping (P_{sp}) palm fruit bunch (PFB) is given as (Khurmi and Gupta, 2012).

$$P_{sp} = \frac{W_{max.s}\, N_s}{60} \quad (6)$$

Where, P_{sp} = power required to drive stripping unit shaft (W) and N_s = rotational speed of stripping unit shaft (rpm).

2.2 Selection of Electric Motor / Generator and Torque

Electric motor that runs at N_1 rpm, was selected based on power required for stripping PFB. Hence, the actual power (P_{actual}) supply is computed as (Antia *et al.*, 2021):

$$P_{actual} = P_{em} \times \eta \quad (7)$$

Where, η = motor power efficiency (%). If the motor is connected to gear reduction box of ratio (G_r : 1), then, the output speed from gear box is N_3 and is computed as:

$$N_3 = \frac{N_1}{G_r} \quad (8)$$

$$T_{em} = \frac{P_{actual} \times 60}{2\pi \times N_3} \quad (9)$$

Where, T_{em} = torque generated at electric motor pulley (Nm) and N_1 = electric motor speed (rpm). Note: 1 hp = 0.745 kW. Consequently, the generator suggested for fabrication should have or same power rating as the electric motor.

2.3 Transmission Drive Design

(a) Design of Pulley

Pulley type chosen was based on the power necessary to drive the shaft.

(b) Determination of Motor Belt Speed

The belt speed and speed ratio are computed as (Khurmi and Gupta (2012).

$$V_3 = \frac{\pi \times d_3 \times N_3}{60} \quad (10)$$

$$\text{Speed ratio} = \frac{N_2}{N_3} = \frac{d_3}{d_2} \quad (11)$$

Where, $V_3 =$ belt speed $(m.s^{-1})$, d_3= diameter of the driver pulley (m), N_3= rotational speed of the driver pulley (rpm), d_2= diameter of the driven pulley (m) and N_2= rotational speed of the driven pulley (rpm).

(c) Determination of Pulley Centre Distance

Minimum (C_{mi}) and maximum (C_{mx}) centre distances considered and are computed as (Khurmi and Gupta, 2012; Antia *et al.*, 2021):

$$C_{mi} = 0.5\,(d_2 + d_1) + d_2 \tag{12}$$

$$C_{mx} = 2\,(d_2 + d_1) \tag{13}$$

Consequently, as shown in Figure 1, the centre distance from the pulleys (C) chosen should be within this range. The nominal length of the belt, L in metres is computed as (Khurmi and Gupta, 2012):

$$L = 2C + \left(\frac{[\pi \times (d_2 + d_1)]}{2}\right) + \left(\frac{[d_1 - d_2]^2}{4C}\right) \tag{14}$$

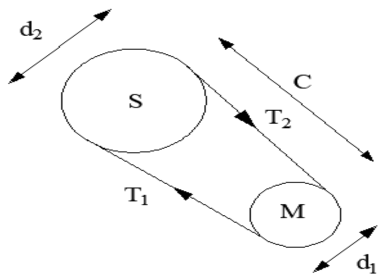

Note: S = shaft pulley, M= motor pulley, T_1 and T_2 are tensions on tight and slack sides respectively.

Figure 1: Pulley centre distance.

(d) Angle of Inclination and wrap of the Belt

The angles of joint and wrap of the belt for an open belt are given thus (Khurmi and Gupta, 2012; Antia *et al.*, 2021):

$$\alpha° = \arcsin\left[\frac{d_1 - d_2}{2C}\right] \tag{15}$$

$$\Theta = [180° - (2 \times \alpha°)]\,\frac{\pi}{180} \tag{16}$$

Where, $\alpha°$ = angle of inclination (^{0}) and Θ = angle of wrap of the belt (rad).

(e) Coefficient of Friction

Coefficient of friction for leather belt on cast iron pulley, at the point of slipping is computed as (Khurmi and Gupta, 2012):

$$\mu_b = \left(0.54 - \left[\frac{42.5}{152.6 + V_1}\right]\right) \tag{17}$$

Where μ_b= coefficient of friction between the belt and the cast iron pulley, and V_1 = belt speed $(m.min^{-1})$.

(f) Cross-Sectional Area (a_b) of the V-belt

The cross-sectional area of the V-belt shall be found by considering areas A, B, and C in Figure 2. The thickness and cross-sectional area of v-belt shall be computed as:

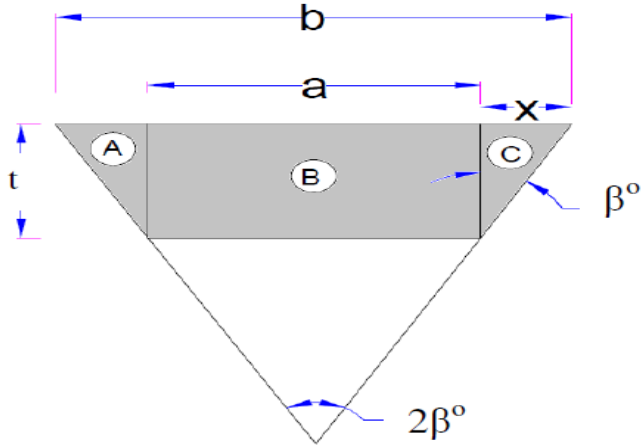

Figure 2: Cross-sectional area of the V-belt.

$$t = \frac{(0.5[b-a])}{\tan \beta°} \quad (18)$$

$$a_b = \text{area of trapezium} = [(b + a)\ 0.5t] \quad (19)$$

Where, t = belt thickness (height) (mm), b = belt top width (mm); a = belt base width (mm), 2β = groove angle for a specific-type of V-belt and a_b = belt cross-sectional area (Khurmi and Gupta, 2012). Hence, maximum and centrifugal tensions in the belt shall be found as (Khurmi and Gupta, 2012):

$$T_{max} = \sigma \times a_b \quad (20)$$

$$T_c = m\ V_1{}^2 = (\rho.\ a_b).\ V_1{}^2 \quad (21)$$

Where, T_m = maximum belt tension (N), σ = maximum allowable stress (2.8 $N.mm^{-2}$), T_c= centrifugal tension in the belt (N), m = mass of belt per unit length (kg), ρ = density of leather belt = 1000 $kg.m^3$, and V_1 = speed of the belt ($m.s^{-1}$).

(g) Belt Tensions, T_1 and T_2

The tension on the tight side of the belt is given as (Khurmi and Gupta (2012):

$$T_1 = T_m - T_c \quad (22)$$

For a V-belt drive, the tension ratio is computed as (Khurmi and Gupta (2012):

$$\left[\frac{T_1}{T_2}\right] = e^{[\mu.\theta \operatorname{cosec} \beta°]} \quad (23)$$

But

$$\operatorname{cosec} \beta° = \frac{1}{\sin\ \beta°} \quad (24)$$

$$T_2 = \frac{T_1}{e^{\left[\mu.\theta\left(\frac{1}{\sin\ \beta°}\right)\right]}} \quad (25)$$

Where, T_1 and T_2 are tensions on the tight and slack sides of the belt, respectively (N).

2.4 Design of Stripping Chamber Shaft

The shaft was designed considering the combined twisting and bending moments. The reactions at the supports for vertical and horizontal loadings was used to obtain maximum vertical bending moment (MBM_V) and maximum horizontal bending moment (MBM_H).

(a) Resultant Bending Moment (M_R)

Resultant bending moment was found as (Khurmi and Gupta, 2012):

$$M_R = \sqrt{(MBM_V)^2 + (MBM_H)^2} \quad (26)$$

(b) Equivalent Twisting Moment (T_e)

The equivalent twisting moment (T_e) was computed as (Khurmi and Gupta, 2012):

$$T_e = \sqrt{(K_m M_R)^2 + (K_t T_{em})^2} \quad (27)$$

Where, T_{em}= torque transmitted by the electric motor (N.m), K_m = combined shock and fatigue factor for bending = 2.0, and K_t = combined shock and fatigue factor for torsion = 1.5 are suggested for suddenly applied load with minor shocks only (Khurmi and Gupta, 2012).

(c) Shaft Diameter (d_s) and Bearing Selection

The shaft diameter was calculated using allowable shear stress (τ) of 42 $N.mm^{-2}$ (Khurmi and Gupta, 2012).

$$d_s = \left[\frac{16T_e}{\tau\pi}\right]^{1/3} \quad (28)$$

Bearing was selected based on the variability and the loads it would carry.

2.5 Key and Keyway Design

The width (W_k), length (L_k) and thickness (t_k) of the key was found using key crushing stress ($\sigma_c = 84\ N.mm^{-2}$), torque conveyed by the shaft (T_{em}) in Equations 29, 30 and 31, respectively (Khurmi and Gupta, 2012; Antia *et al.*, 2021).

$$W_k = \frac{d_s}{4} \quad (29)$$

$$L_k = \frac{2 \times T_{em} \times 1000}{W_k\ \tau\ d_s} \quad (30)$$

$$t_k = \frac{4 \times T_{em} \times 1000}{L_k\ d_s\ \sigma_c} \quad (31)$$

2.6 Design of Bolts and Nuts

The bolt and nut were designed based on the consideration to the shear stress on the machine (Antia *et al.*, 2021).

$$d_b = \sqrt{\frac{4 \times W_{t.max}}{\pi\ S_e}} \quad (32)$$

Where, d_b = bolt diameter (mm), S_e= allowable endurance stress of mild steel (107.696 × 10^3 $kN.m^{-2}$), $W_{t.max}$ = assumed maximum total load on the machine (kN).

2.7 Fruitlet Screen Design

As shown in Figure 3, the screen aperture (a_{screen}) was designed in such way that the major dimension of the biggest palm fruit of any variety ($D_{m.f}$) can pass through but at the same time not allowing the threshed spikelet of any dimension ($D_{spikelet}$) to go through. By using inequality, we have,

$$D_{m.f} \leq a_{screen} < D_{spikelet} \tag{33}$$

Where, a_{screen} = a

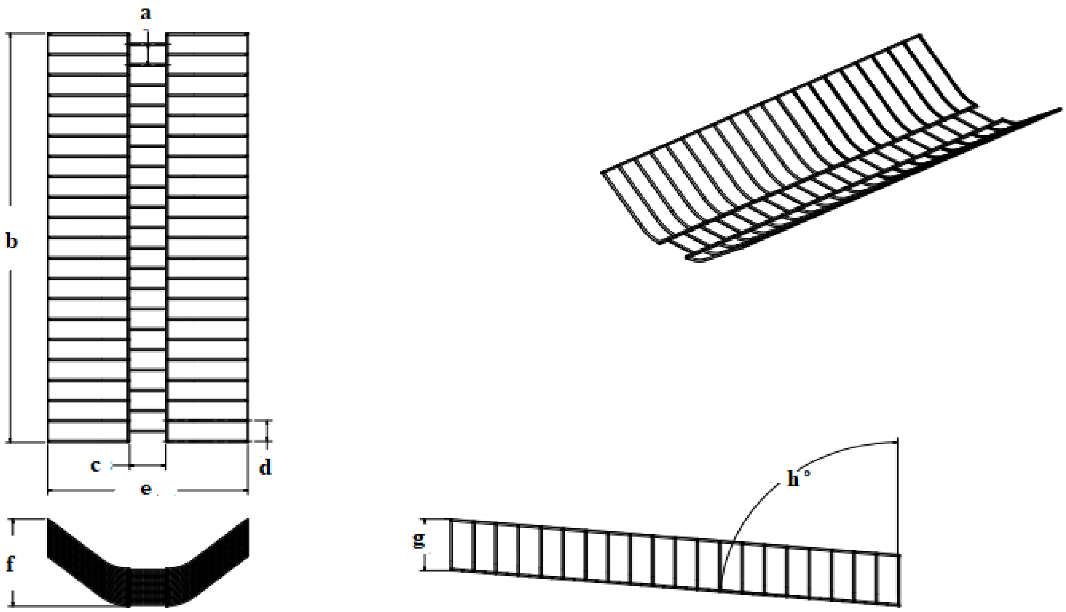

Figure 3: The Sieve

(a) Number of Rods (150 mm Thickness)

Number of rods with 150 mm thickness is given as:

$$n_{rod} = \frac{L_{cb} - (S_n \, . \, S_{rod})}{t_{rod}} \tag{34}$$

Where, n_{rod} = number of rods, L_{cb} =length of sieve (m), S_n = number of empty spaces, S_{rod} = space between rods (m) and t_{rod} = thickness of rod (m).

(b) Total length of Trapezoidal Shape Rod

Total length of trapezoidal shape rod (T_{L-rod}) as shown in Figure … is given as

$$T_{L-rod} = [(2 \times \text{slant height}) + \text{base}] \text{ per trapezoidal section } n_{rod} \tag{35}$$

2.8 Stripping Chamber Design

The body cover of the stripping chamber is shown in Figure 4.

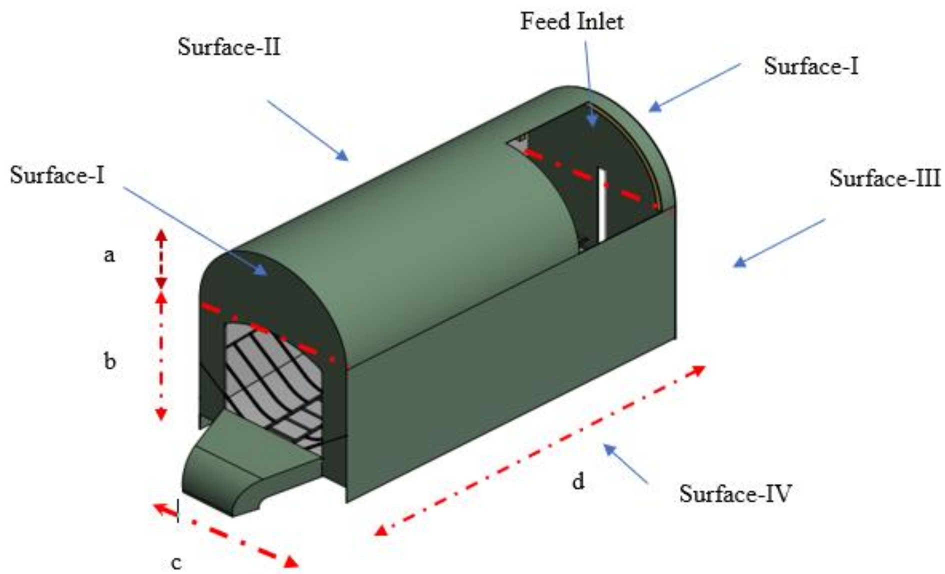

Figure 4: Body cover.

(a) Surface Area of Body Cover

The surface area of body cover (S_{bc}) is given as:

$$S_{bc} = \text{area}\ (2\text{I}) + \left(\frac{5\ \text{II}}{6}\right) + \text{III} + (2\text{IV}) \quad (36)$$

Where;

$$\text{Semicircular surface I} = \frac{\pi\ a^2}{2} \quad (37)$$

$$\text{Semi curve circular surface II} = \pi\ a\ d \quad (38)$$

$$\text{Square surface III} = b \times c \quad (39)$$

$$\text{Rectangular surface IV} = b \times d \quad (40)$$

$$\text{Feed inlet area} = \frac{\text{II}}{6} \quad (41)$$

Also, a = radius of semi-circular segment (m), b= height of the square segment (m), c= width of the chamber (m) and d= length of the chamber (m).

(b) Capacity of the Stripping Chamber (C_{sc})

The capacity of the stripping chamber (C_{sc}) is computed as:

$$C_{sc} = (bcd) + (0.5\ \pi a^2 d) \quad (42)$$

2.9 Frame Design

Frame was designed to support the load on the machine. It composes of an iron arc stand, angle bars (t = thickness = 0.005 m and w = width 0.075 m) and rectangular bars (0.05 by 0.05 m) as shown in Figure 5.

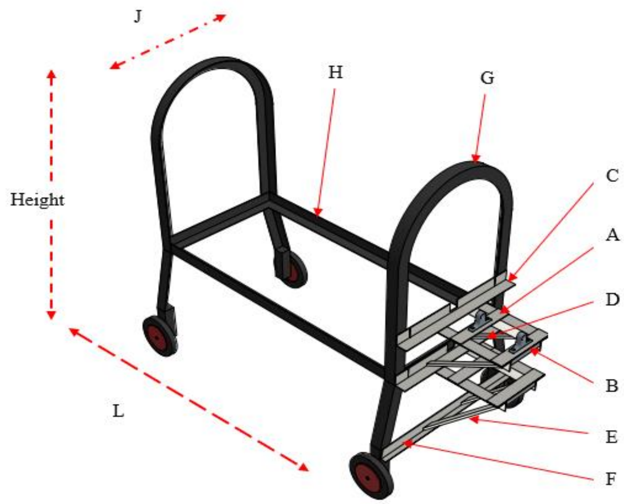

Figure 5: Frame structure.

(a) Arc Stand

$$\text{Length of arc} = \frac{180^0\ 2\pi\ a}{360^0} = \pi\ a \tag{43}$$

Height = ɧ m and distance between adjacent wheels = ƴ m.

(b) Dimensions of Angle and Rectangular Bars

The dimensions of the angle and rectangular bars in the frame structure of Figure 5 are shown in Table 1.

Table 1: Dimensions of angle and rectangular bars

Part	Name	Dimensions (m)	Pieces
A	Frame (angle bar)	L = 0.30	4
B	Frame (angle bar)	L = 0.30	4
C	Frame (angle bar)	L = 0.50	2
D	Frame support (angle bar)	L = 0.58	2
E	Frame support (angle bar)	L = 0.71	2
F	Frame support (angle bar)	L = 1.01	1
G	Arc frame		2
H	Rectangular frame support	e_1 by e_2	
J	Diameter of the Semi circle		2

3.

Results and Discussion

The design calculations were conducted using Customized M236 Machine Design Spreadsheet, powered by Microsoft Excel®. The relevant input parameters were provided and the design calculations were conducted based on the expressions presented as Equation 1 to Equation 43.

3.1 Input parameters and results on the selection of the power requirement for stripping Process (P_{sp})

The parameters and their corresponding variables used in the computation of the power required for the stripping process are shown in Table 2. According to the data in Table 2, two bunches of palm fruits each weighing 40 kg were considered in the calculation and the result obtained for the power expected for stripping process was 2.218 kW or 2.98 hp.

Table 2: Computation of power requirement for stripping process

Parameter	**Symbol**	**Value**	**Unit**
Acceleration due to gravity	g	9.81	m/s^2
Mass of oil palm fruit bunch	m_{fb}	40	kg
Number of palm fruit bunches in the stripping chamber	n_f	2	
Weight of n-number of oil palm fruit bunch	W_{nf}	784.8	N
Height of beater blade	h	0.0887	m 0.04667
Base of beater blade	b	0.0300	m
Length of beater blade	l	0.0500	m
Volume of a beater blade	V_{bb}	0.0000 7	m^3
Density of beater blade (mild steel)	ρ	7860	kg/m^3
Number of spots	n_{-spot}	12.00	
Each spot has q-number of beater blades	q	4.00	
Total number of beater blades	$t_{-blades}$	48.00	
Weight of total number of beater blades	$W_{t-blades}$	246.22	N
Stripping force after 24 hours of storage (Olotu *et al.* 2020)	F_{sp}	300.0	N
Maximum load key on the shaft	$W_{max.s}$	1331.0 2	N
Maximum speed of the shaft	N_s	100	rpm
Power expected for stripping process	P_{sp}	2218.3 6	W
	p_{sp}	2.218	kw
note 1 hp = 0.745 kw		2.98	hp

3.2 Input parameters and results on the selection of the electric motor power, generator and torque

Parameters used in selecting electric motor power are shown in Table 3.According to the results in Table 3, the electric motor power supply (to be chosen) is 5.33 hp, the speed from gear box is 100 rpm and the torque on shaft or the machine pulley is 284.53 N-m.

Table 3: Selection of electric motor power, generator and torque

Parameter	Symbol	Value	Unit
Actual electric motor power supply	P_{ac}	4.00	hp
Assume the electric motor efficiency (ɳ)	ɳ	0.75	
Electric motor power supply (to be chosen)	P_{em}	5.33	hp
Rotational speed of the electric motor (chosen)	N_1	1500	rpm
Gear box (speed reducer) (15:1)	G_r	15	
Speed from gear box	N_3	100.0	rpm
Power equivalent supplied to shaft (1 hp = 0.745kW)	P_{ac}	2980.0	W
Torque on shaft or the machine pulley	T_{em}	284.53	N-m

3.3 Input parameters and results on the selection of the transmission drive

Input parameters and results on the selection of the transmission drive are shown in Table 4. According the design parameters shown in Table 4, the actual speed (speed of rotation of the driven pulley) is the same 100 rpm with the speed of rotation of the driver pulley which means that speed ratio of 1 is used in the design. The results also showed that the groove angle for the (A)-type V-belt used is β = 17 degrees.

Table 4: Selection of transmission drive

Parameter	Symbol	Value	Unit
Speed of rotation of the driven pulley (actual speed)	N_2	100.0	rpm
Speed of rotation of the driver pulley	N_3	100.0	rpm
Diameter of the driver pulley	d_3	0.060	m
Diameter of driven pulley	d_2	0.060	m
Speed of the belt	V_3	0.31	m/s
Speed ratio		1.0	
Minimum center distance	C_{mi}	0.120	m
Centre distance from the pulleys (selected)	C	0.120	m
Nominal length of the belt	L	0.429	m
Sin α°		0.000	
Joint angle	α°	0.0000	degrees
Angle of contact	ϴ	3.14	rad
Speed of belt in (metres/min)	V_3	18.85	m/min.
Coefficient of friction	μ	0.29	

Maximum allowable stress	σ	2.8	N/mm^2
Top width of the belt	b	13.0	mm
Base width of the belt	a	8	mm
Groove angle for (A)-type V-belt, 2β = (34 degrees)	β	17	degrees
	Tan β	0.3058	
Cross-sectional area of the V-belt	a_b	85.85	mm^2

3.4 Input parameters and results on the selection of the belt tensions

The input parameters and results on the selection of the belt tensions are shown in Table 5. Notably, the tensions on the tight and slack sides of the belt are 240.37 N and 10.42 N respectively.

Table 5: Input parameters and results on the selection of the belt tensions

Parameter	Symbol	Value	Unit
Density of V-belt	ρ	1000	kg/m^3
Maximum tension in the belt	T_m	240.38	N
Centrifugal tension in the belt	T_c	0.0085	N
Tension on the tight side of the belt	T_1	240.37	N
Tension on the slack side of the belt	T_2	10.42	N

3.5 Input parameters and results on the selection of the total weight at the pulleys

Input parameters and results on the selection of the total weight at the pulleys are shown in Table 6.

Table 6: Total weight at the pulleys

		Vertical Force	Horizontal Force	
Parameter	**Symbol**	**Value**	**Value**	**Unit**
Weight of pulley(s)	W_p	3.20	0.00	N
Joint angle	**α°**	0.00	0.00	degrees
Tension on the tight side of the belt	T_1	240.37	240.37	N
Tension on the slack side of the belt	T_2	10.74	10.74	N
Total weight at the pulley (G)	W_{tp}/T_p	3.20	251.11	N
Weight at B	$W_{max.s}$	1331.02	0.00	N

3.6 Maximum Bending Moment

Bending moments in the vertical and horizontal planes are shown in Figure 5 and Figure 6. As shown in Figure 5, reactions at point A, B, C, D, E and F were 444.20, -1331.02, 2805, -2585, 669.20 and -3.20 N, respectively whereas the maximum bending moment in vertical plane was found at point (MBM_V) C as 442.7 N-m. However, the negative sign means that the force is acting vertically downward. Also, in Figure 6, reactions at point A, C, D, E and F were 0.17, 18.4, -169.4, 402.3 and -25.1 N, respectively while the maximum bending moment in horizontal plane was at point (MBM_H) E as 25.1 N-m. This implies that more support should be given at point of maximum bending moment.

Based on the parameters in Table 6, resultant bending moment ($M_R = 443.41\ N - m$) was found. This was used alongside torque transmitted by the motor (284.53 N-m), combined shock and fatigue factor for bending (2.0) and combined shock and fatigue factor for torsion ($K_t = 1.5$) to simulate equivalent twisting moment ($T_e = 984.18\ N - m$). Allowable shear stress ($\tau = 42$ N/ mm^2) was incorporated to compute shaft diameter of 47. 4 mm (50 mm selected).

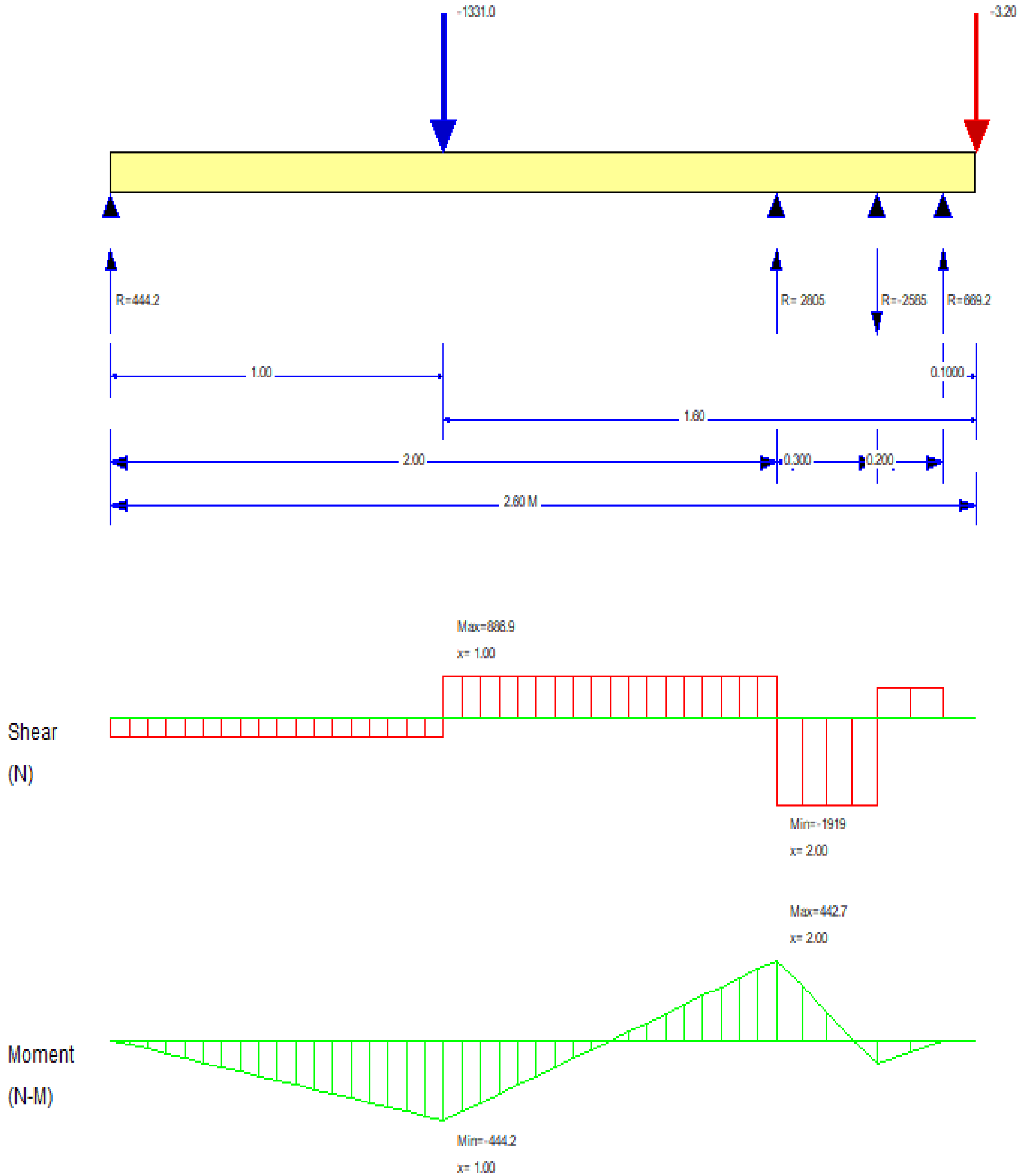

Figure 5: Torsional and bending moment diagram in the vertical plane.

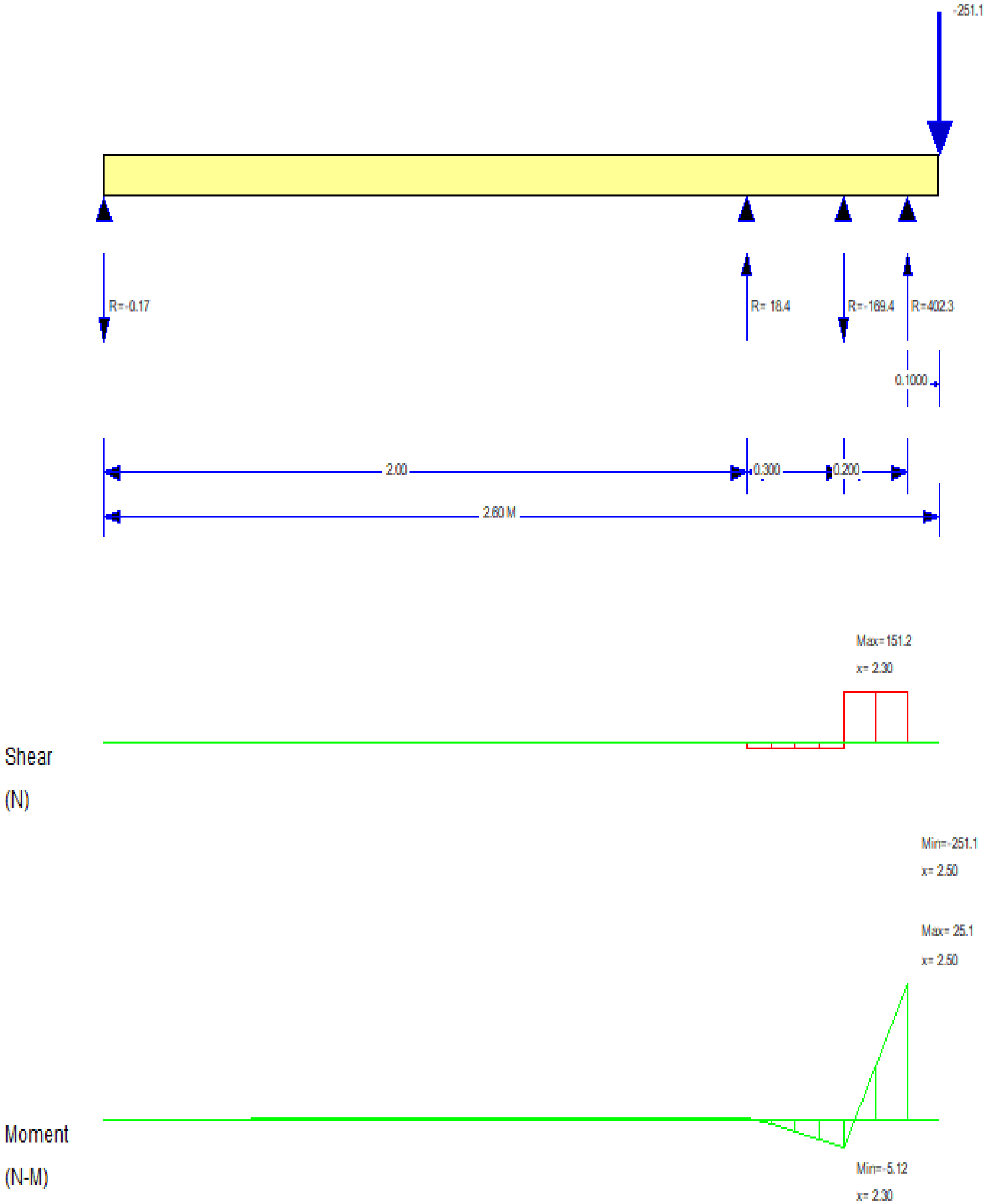

Figure 6: Torsional and bending moment diagram in the horizontal plane.

3.7 Input parameters and results on the selection of the shaft

Shaft was selected based on the computation presented in Table 7.

Table 7: Shaft selection

Parameter	**Symbol**	**Value**	**Unit**
Resultant bending moment	M_R	443.41	N-m
Torque transmitted by the motor	T_{em}	284.53	N-m
Combined shock and fatigue factor for bending	K_m	2.0	
Combined shock and fatigue factor for torsion	K_t	1.5	
Equivalent twisting moment	T_e	984.18	N-m
Allowable shear stress	τ	42	N/mm^2
Shaft diameter	d_s	47.4	mm
Shaft diameter selected	d_s	50	mm

3.8 Input parameters and results on the selection of the keyway, bolt and bearing

Input parameters and results on the computation for the selection of keyway, bolt and bearing is shown in Table 8.

Table 8: Keyway, bolt and bearing selection

Parameter	**Symbol**	**Value**	**Unit**
Key and Keyway:			
Crushing stress of the key	σ_c	84	N/mm2
Width of the key	W_k	12.5	mm
Length of the key	L_k	21.7	mm
Thickness of the key	t_k	12.5	mm
Maximum endurance stress of mild steel	S_e	107696	kN/m^2
Assumed max. load on the system	$W_{t.max}$	10	kN
Bolt diameter	d_b	0.01087	m
	d_b	10.87	mm
Selected bolt diameter	d_b	10	mm
Bearing Selection			
Bearing bore diameter		40 - 50	mm

3.9 Input parameters and results on the fruitlet screen design, the stripping chamber design

For the design of the fruitlet screen design, from Figure 3; b = 2 m; a_{screen} = a = d = 0.03 m = 0.03 m; c* = 0.15 m; e = 0.45 m; f= 0.3 m; g = 0.20 m and h= 85^0.

L_{cb} = length of sieve = 2 m

S_n = number of empty spaces = 50

S_{rod} = space between rods = 0.03 m

n_{rod} = number of rods (150 mm thickness) (33.3 ≈ 33 rods)

Slant height (0.33 m)

Base (0.15 m)

T_{L-rod} = 26.73 m

For the design of the stripping chamber design calculations, from Figure 4; a = 0.4 m, b = 0.6 m, c= 0.5 m, d = 2 m, then,

S_{bc} = surface area of body cover = 5.297 m^2

C_{sc}= capacity of the stripping chamber = 1.10272 m^3

For the design of the frame design calculations, from Figure 5, (t = thickness = 0.005 m and w = width 0.075 m and rectangular bars be 0.05 by 0.05 m)

Length of arc = 1.2568 m

Height = ɧ m = 1.5 m

Distance between adjacent wheels = ƴ m = 1.0 m

The dimensions of angle and rectangular bars is given in Table 9.

Table 9: Dimensions of angle and rectangular bars.

Part	**Dimensions (m)**	**Pieces**	**Total Length (m)**
Angle Bar			
A	L = 0.30	4	1.20
B	L = 0.30	4	1.20
C	L = 0.50	2	1.00
F	L = 1.01	1	1.01
H	e_1 by e_2 = 2.0 × 0.5	1	5.00
G	(1.4 m × 4 arms) + (2 × L-arc)		8.11
		Total	17.52
Rectangular Bar			
D	L = 0.58	2	1.16
E	L = 0.71	2	1.42
		Total	2.58

As shown in Figure 3, the fruitlet screen resembles a slopy valley. It is expected to be 2 m long, with 0.03 m rods apart to allow the fruits fall down the receptacle. The screen design (fruit outlet) of Onifade *et al.* (2016) was 20 mm diameter rod by 20 mm square holes. A total number of 50 spaces shall be created. The slant height of the valley-shape sieve should be 0.33 m each with 0.15 m depression. The total length of the rod be used was computed as 26.73 m. The capacity of the stripping chamber (Figure 4) is 1.10272 m^3 whereas the stripping chamber designed by Onifade *et al.* (2016) was 0.00027 m^3. The frame (Figure 5) of this study design should be made of angle of 0.05 thickness and 0.075 width; and rectangular bars of 0.05 by 0.05 dimensions. The length of the arc is 1.2586 m while height of the frame is 1.5 m. The total of angle bar to be used is 17.52 m while that of rectangular bar is 2.58 m.

4. Conclusion

The detailed design procedure is presented for a movable palm fruit bunch stripper (MPFBS) plant for oil extraction is presented. The relevant analytical models for the calculation of the various component parameters are also presented. Sample design calculations were conducted using Customized M236 Machine Design Spreadsheet, powered by Microsoft Excel®. Among other things, the design calculations included determination of the power requirement for stripping operation, selection of the transmission drive and belt tensions parameter values, the total weight at the pulleys, bending moments, selection of the shaft, as well as the fruitlet screen and the stripping chamber design parameters values.

References

Adade, F. B. (2022). Oil Palm (Elaeis guineensis) Cultivation and Food Security in the Tropical World. *Elaeis guineensis*, 171.

Antia, O. O., Assian, U. E., & Ukaru, Y. N. (2021). Design and fabrication of a modified fish feed pelletizing machine. *Global Journal of Engineering and Technology Advances*, *7*(2), 001-011.

Antia, O.O., Assian, U. E. and Ukaru, Y. N. (2021). Design and fabrication of a modified fish feed pelletizing machine. Global Journal of Engineering and Technology Advances, 7(2): 1 - 11. Available Online at https://doi.org/10.30574/gjeta.2021.7.2.0063. IF = 5.78

Asbur, Y., Purwaningrum, Y., & Ariyanti, M. (2020). Vegetation Composition and Structure under Mature Oil Palm (Elaeis guineensis Jacq.) Stands. In *Proceedings of the 7th International Conference on Multidisciplinary Research (ICMR 2018)* (pp. 254-260).

Assian, U. E., Okoko, J. U., Alonge, F. A., Udoumoh, U. I. and Ehiomogue, P. (2022). Development of Sustainable Products from Oil Palm Towards Enhancing National Food Security: A Review. Scientific Journal, Agricultural Engineering, University of Belgrade, Faculty of Agriculture, Belgrade-Zemun, 1: 15 -35

Babu, B. K., Mathur, R. K., Anitha, P., Ravichandran, G., & Bhagya, H. P. (2021). Phenomics, genomics of oil palm (Elaeis guineensis Jacq.): way forward for making sustainable and high yielding quality oil palm. *Physiology and Molecular Biology of Plants*, *27*, 587-604.

Gan, S. T., Teo, C. J., Manirasa, S., Wong, W. C., & Wong, C. K. (2021). Assessment of genetic diversity and population structure of oil palm (Elaeis guineensis Jacq.) field genebank: a step towards molecular-assisted germplasm conservation. *Plos one*, *16*(7), e0255418.

Khurmi, R. S. and Gupta, J. K. (2012). *A Text Book of Machine Design*. Eurasia Publishing House (PVT.) Ltd, Ram Nagar, New Delhi, 1230p.

Mayes, S. (2020). The history and economic importance of the oil palm. *The Oil Palm Genome*, 1-8.

Nair, K. P., & Nair, K. P. (2021). Oil Palm (Elaeis guineensis Jacquin). *Tree Crops: Harvesting Cash from the World's Important Cash Crops*, 249-285.

Olosunde, W. A., Assian, U. E., & Antia, O. O. (2023). Determination of Rotor Operating Factor (Efficiency) Required for the Design of Rotor Speed in a Centrifugal Nut Cracker. *American Journal of Innovation in Science and Engineering*, *2*(2), 26-30.

Oshiobugie, M., Atumah, E. V, Nnabuife, A., Ariavie, G. O. and Sadjere, E. G. (2017). *Design of a Palm Bunch Stripping Machine Suitable for use in Benin City , Edo State , Nigeria*. *7*(5), 413–417.

Oteng, A. (2020). *Livelihood Vulnerability and Adaptive Capacity of Smallholder Oil Palm Farmers in Kwaebibirem Municipality of Ghana* (Doctoral dissertation, University of Cape Coast).

Pinnamaneni, R., & Potineni, K. (2022). Integrated Pest Management (IPM) in Oil Palm, Elaeis guineensis Jacq. In *Palm Oil-Current Status and Updates*. IntechOpen.